The spontaneous resistivity anisotropy in Ni-based alloys

The spontaneous resistivity anisotropy in Ni-based alloys

I. A. CAMPBELL, A. FERT and O. JAOUL

Physique des Solides†, Faculté des Sciences, 91-Orsay, France
MS. received 22nd December 1969

Abstract. From experiments on a number of Ni-based alloys, it is shown that the difference in resistivity for currents perpendicular to and parallel to the magnetization direction is due to spin–orbit induced resistivity transfer from the spin-down electron current to the spin-up electron current.

1. Introduction

It has been known for over a century that there exists a spontaneous resistivity anisotropy associated with the magnetization in ferromagnetic metals. A number of different mechanisms have been proposed (Smit 1951, Berger 1964, Vu Dinh Ky 1967) to explain this phenomenon, all depending on spin–orbit coupling. In this paper we show that a model we have proposed (Campbell 1970) based on the mechanism of Smit (1951) and on parallel current conduction (Campbell, Fert and Pomeroy 1967, Fert and Campbell 1968) explains in considerable detail the experimental results on the resistivity anisotropy in Ni and Ni-based alloys.

2. Model

The density-of-states curves in Ni for spin ↑ and spin ↓ electrons are shown schematically in figure 1. At the spin ↑ Fermi surface there are only conduction electron states, while at the spin ↓ surface there are d states as well as conduction electron states. For simplicity we will from now on refer to the conduction electron states as s states.
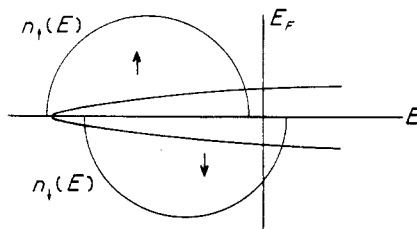

Figure 1. Schematic band structure of Ni; densities of states of d (humped) and s bands.

Transport at low temperatures in the absence of spin–orbit coupling but in the presence of impurities is by two parallel currents of electrons, spin ↑ and spin ↓, each with its own 'residual resistivity', $\rho_\uparrow^0$ and $\rho_\downarrow^0$. The values of these parameters have been measured for a number of impurities in Ni (Fert and Campbell 1968, Farrell and Greig 1968) by comparing low and high-temperature resistivities of samples containing a given impurity, or by measurements at low temperatures on samples containing two impurities simultaneously. The ratio $\rho_\downarrow^0/\rho_\uparrow^0$ is called α, and is fixed for a given impurity, independent of temperature or concentration (as long as temperatures are well below the Curie temperature T_c, and the
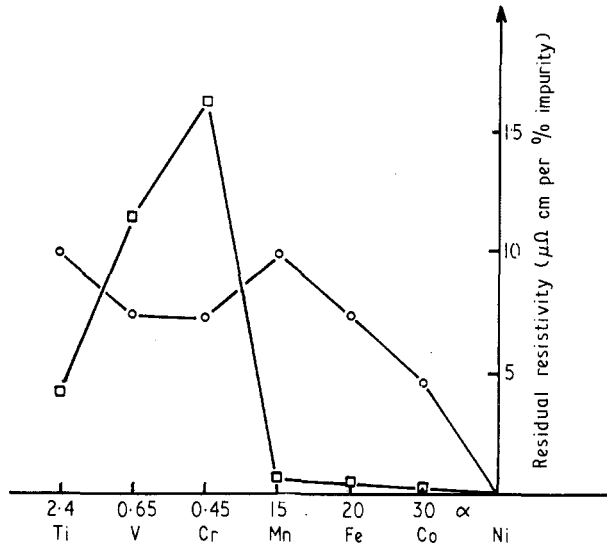
† Laboratoire associé au CNRS.

Figure 2. Experimental values of $\rho_\uparrow^0$ ($\square$), $\rho_\downarrow^0$ ($\bigcirc$) for the first-series impurities in Ni. The resistivities are in $\mu\Omega$ cm per % impurity.
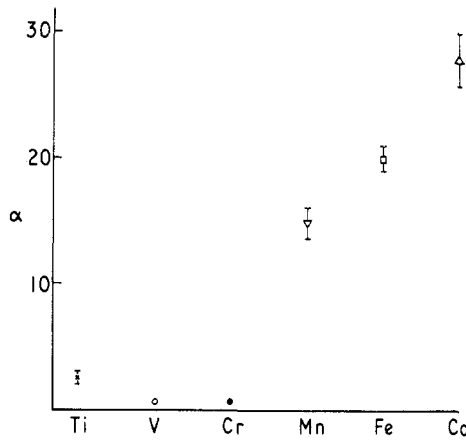

Figure 3. Values of $\alpha = \rho_\downarrow^0/\rho_\uparrow^0$ for first-series impurities in Ni.

concentrations such that the impurity atoms scatter independently). The values of $\rho_\uparrow^0, \rho_\downarrow^0$ and α for first-series impurities in Ni are given in figures 2 and 3. The peak in $\rho_\uparrow^0$ at Cr is associated with a d$\uparrow$ bound state close to the Fermi energy (Friedel 1958).

As the temperature is increased, additional terms $\rho_\uparrow^P(T)$, $\rho_\downarrow^P(T)$ must be added to the spin $\uparrow$ and spin $\downarrow$ resistivities respectively, and a spin mixing term due to magnons (Fert 1969) $\rho_{\uparrow\downarrow}(T)$ appears. These three resistivities are characteristic of the host only and do not depend on the impurity. The ratio $\rho_\downarrow^P(T)/\rho_\uparrow^P(T)$ is called μ. The general expression for the total resistivity is

$$\rho(T) = \frac{\rho_\uparrow\rho_\downarrow + \rho_{\uparrow\downarrow}(\rho_\uparrow + \rho_\downarrow)}{\rho_\uparrow + \rho_\downarrow + 4\rho_{\uparrow\downarrow}} \tag{1}$$

where

$$\rho_\sigma = \rho_\sigma^0 + \rho_\sigma^P(T).$$

In the absence of spin–orbit coupling, there are no d band states at the Fermi level for spin ↑, so all scattering processes are from s↑ states to s↑ states, possibly passing through a bound d↑ state (Cr or V impurities). For s↓ scattering, there are additional processes ending in d↓ band states. Calculations (Gomes 1966) show that s–d processes (if they are permitted) normally dominate over s–s processes; experimentally, for phonons or most impurities, $\rho_\downarrow$ (which includes s–d and s–s) is greater than $\rho_\uparrow$ (s–s only). Exceptions occur when there is a d resonance near the spin ↑ Fermi energy (Cr, V).

Now, in the presence of spin–orbit coupling in the d band, a certain amount of d↑ character is mixed into the d↓ band, and *vice versa*; in particular, there will be some d↑ character mixed into the d↓ states at the Fermi surface. This permits s↑ scattering into the d↑ part of the mainly d↓ Fermi surface. The d↑–d↓ mixing is not isotropic because the magnetization direction provides an axis for the spin–orbit perturbation, so it provides a mechanism for the resistivity anisotropy. The d↑–d↓ mixing will be discussed in § 3, and application to the two-current model will be made in § 4, where we show that the resistivity anisotropy depends essentially on the ratio of spin ↑ to spin ↓ currents. In § 5 experimental results are presented for various alloys.

3. Spin–orbit interaction

We will follow what is essentially the argument of Smit (1951). Suppose we take a tight binding model for the d states, and we assume there is an exchange field $H_z^e S_z$ but no crystal field, so that, without spin–orbit coupling, for each spin the five d states have the identical densities of states and have spatially the form of the atomic d functions. The spin–orbit perturbation is

$$A \, \mathbf{L}.\mathbf{S} = A\{L_z S_z + \tfrac{1}{2}(L_+ S_- + L_- S_+)\}$$

where A is small compared to H_z^e. The first term lifts the degeneracy of the d states of a given spin, but will be neglected from now on. The spin ↓ wave functions become

$$
\left.
\begin{aligned}
\Psi|2\downarrow\rangle &= (1 - \tfrac{1}{2}\epsilon^2)\,\phi|2\downarrow\rangle + \epsilon\phi|1\uparrow\rangle \\
\Psi|1\downarrow\rangle &= (1 - \tfrac{3}{4}\epsilon^2)\,\phi|1\downarrow\rangle + (\tfrac{3}{2})^{1/2}\epsilon\phi|0\uparrow\rangle \\
\Psi|0\downarrow\rangle &= (1 - \tfrac{3}{4}\epsilon^2)\,\phi|0\downarrow\rangle + (\tfrac{3}{2})^{1/2}\epsilon\phi|-1\uparrow\rangle \\
\Psi|-1\downarrow\rangle &= (1 - \tfrac{1}{2}\epsilon^2)\,\phi|-1\downarrow\rangle + \epsilon\phi|-2\uparrow\rangle \\
\Psi|-2\downarrow\rangle &= \phi|-2\downarrow\rangle
\end{aligned}
\right\} \quad (2)
$$

where $\epsilon = A/H_z^e$.

If we assume that the s electrons are plane waves, and that the s–d scattering potential is spherical, we can calculate very simply the s–d transition probabilities for s electrons with different directions of $\mathbf{k}$. If we write the orientation functions of the different d orbitals

$$
\begin{aligned}
m &= \pm 2 & (1/2\sqrt{2})(x \pm iy)^2 \\
m &= \pm 1 & (1/\sqrt{2})\,z(x \pm iy) \\
m &= 0 & (1/\sqrt{12})(r^2 - 3z^2)
\end{aligned}
\quad (3)
$$

then it can be seen that, for example, the state $\exp(i\mathbf{k}_z.\mathbf{r})$ can only be scattered into the d state $m = 0$, and $\exp(i\mathbf{k}_x.\mathbf{r})$ into the states $m = \pm 2, 0$, with appropriate coefficients in each case. It is easily shown from (2) and (3) that

$$
\begin{aligned}
\rho_{sd}^\uparrow(k_z) &= \tfrac{3}{2}\epsilon^2\rho' \\
\rho_{sd}^\uparrow(k_x) &= \tfrac{3}{4}\epsilon^2\rho' \\
\rho_{sd}^\downarrow(k_z) &= (1 - \tfrac{3}{2}\epsilon^2)\,\rho' \\
\rho_{sd}^\downarrow(k_x) &= (1 - \tfrac{3}{4}\epsilon^2)\,\rho'
\end{aligned}
\quad (4)
$$

where ρ' is the s–d resistance for spin ↓ electrons in the absence of spin–orbit coupling.

E

This calculation is obviously greatly over-simplified, but shows the essential properties of the mechanism, which is that a part of $\rho_\downarrow$ is transferred to $\rho_\uparrow$, this effect being about twice as strong for electrons travelling along the magnetization direction as for those travelling perpendicular to it.

4. Effect on the resistivity

In order to have a formula that we can apply directly to experimental results, we shall make two further approximations. First, we will assume *all* $\rho_\downarrow$ is due to s–d scattering. Secondly, we will assume the magnon scattering is not affected by spin–orbit coupling. Following (4) we write

$$\rho_\parallel^\uparrow = \rho_\perp^\uparrow + \gamma\rho_\perp^\downarrow$$
$$\rho_\parallel^\downarrow = \rho_\perp^\downarrow - \gamma\rho_\perp^\downarrow \qquad (5)$$
$$\rho_\parallel^{\uparrow\downarrow} = \rho_\perp^{\uparrow\downarrow}$$

where $\parallel$ and $\perp$ refer to the magnetization direction, and γ is a constant independent of the scattering process. Even though the preceding calculation is very rough, it justifies this set of equations, and should give an estimate of $\gamma \simeq \frac{3}{4}\epsilon^2$.

Putting these relations (5) into (1), we have

$$\frac{\Delta\rho}{\rho} = (\rho_\parallel - \rho_\perp)\frac{1}{\rho_\perp} = \frac{\gamma(\rho_\downarrow - \rho_\uparrow)\rho_\downarrow}{\rho_\uparrow\rho_\downarrow + \rho_{\uparrow\downarrow}(\rho_\uparrow + \rho_\downarrow)} \qquad (6)$$

and in particular at low temperatures

$$\frac{\Delta\rho}{\rho} = (\alpha - 1)\gamma. \qquad (7)$$

The general behaviour to be expected from these expressions is as follows. At low temperatures, $\Delta\rho/\rho$ should be proportional to the quantity $\alpha - 1$ characteristic of the dominant impurity and independent of impurity concentration. At higher temperatures, values of $\Delta\rho/\rho$ for dilute alloys should tend to that of the pure metal, converging the faster as their concentrations are lower. Experimental results follow these predictions very closely, as we will show in the next section.

5. Experimental results

It should be noticed first of all that we have not taken into account effects in which the magnetic field acts directly on the electron trajectories. This means that $\rho_\parallel$, $\rho_\perp$ values should be taken from experimental results extrapolated back to $B = 0$. In practice this is a small correction for sample resistivities greater than 1 $\mu\Omega$ cm. An extensive table of results is given by van Elst (1959), unfortunately often at rather high minimum concentrations. We have measured samples of NiCo, NiFe, NiMn and NiCr, at concentrations below 3%.

(i) Figure 4 presents low-temperature results for NiMn, NiFe, and NiCr as a function of impurity concentration. This shows that the prediction of $\Delta\rho/\rho$ being independent of concentration is essentially correct.

(ii) Again at low temperatures, $\Delta\rho/\rho$ is plotted against α in figure 5 for different impurities. The α values were of course determined from zero-field resistance measurements without any reference to $\Delta\rho/\rho$ values. Agreement with (7) is excellent. The value of γ which best fits the slope is

$$\gamma \simeq 0.0075$$

(iii) Figures 6 and 7 show calculated and experimental values of $\Delta\rho/\rho$ for different impurities as functions of concentration at 77°K and 293°K. The same impurity α values and the value of γ deduced from the low-temperature measurements were used for the calculated
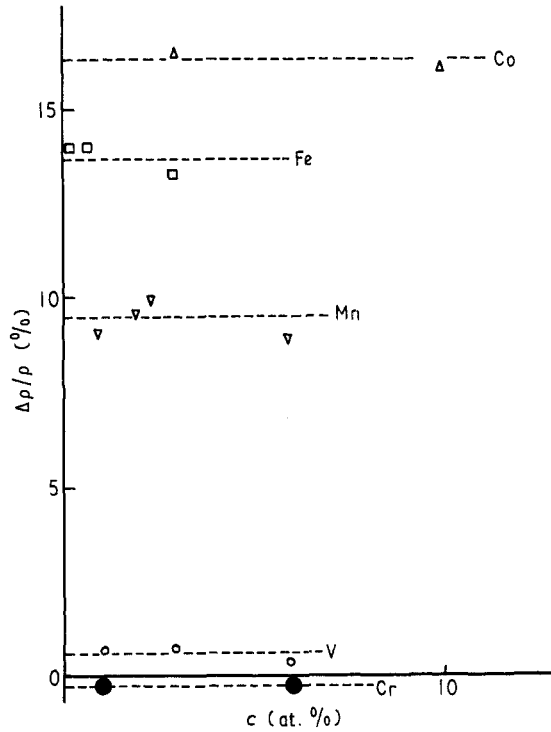
Figure 4. Experimental low-temperature values of $\Delta\rho/\rho = (\rho_{\parallel} - \rho_{\perp})/\rho_{\perp}$ as a function of impurity concentration c (at.%). Values are for 4·2 K, except for values taken from van Elst (1959) which are for 14 K. $\triangle$ Cobalt; $\square$ Iron; ∇ Manganese; $\bigcirc$ Vanadium; $\bullet$ Chromium.
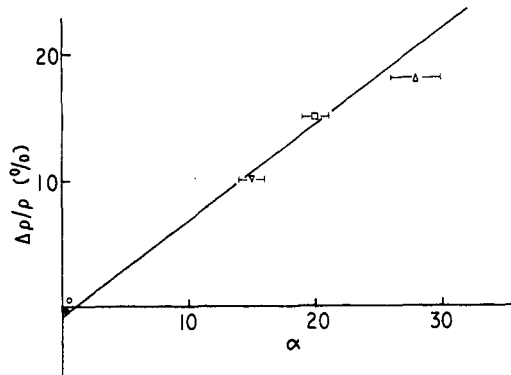

Figure 5. Experimental values of $\Delta\rho/\rho$ from figure 4 plotted against α values from figure 3. Straight line is for $\Delta\rho/\rho = 0·0075 \, (\alpha - 1)$.

curves. The parameters μ and $\rho_{\uparrow\downarrow}$ have not been determined accurately by resistivity measurements at these temperatures, but the values (chosen to fit $\Delta\rho/\rho$ for the pure metal) are not inconsistent with previous estimates.

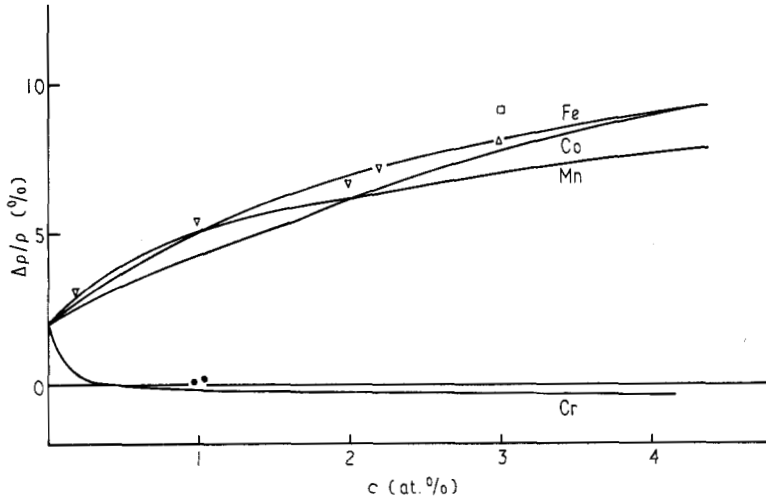It can be seen that the fit is again satisfactory.

Figure 6. Experimental results and calculated curves for 77 K. Curves calculated with the $\rho_\uparrow^0$, $\rho_\downarrow^0$ values given above, $\gamma = 0.0075$, $\mu = 5$ and $\rho_{\uparrow\downarrow} = 0.33\ \mu\Omega$ cm.
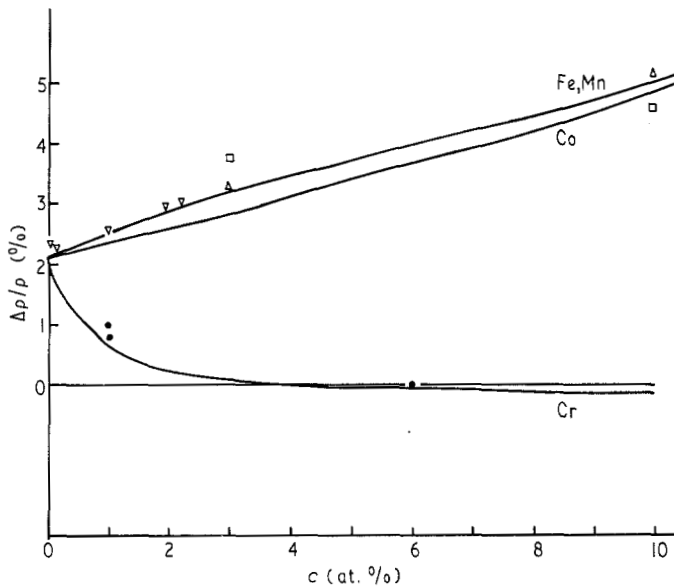

Figure 7. Experimental results and calculated curves for 293 K. Curves calculated with $\rho_\uparrow^0$, $\rho_\downarrow^0$ values given above, $\gamma = 0.0075$, $\mu = 5$ and $\rho_{\uparrow\downarrow} = 3.0\ \mu\Omega$ cm.

6. Value of λ

It is possible to make an independent estimate of the value expected for γ from the gyromagnetic ratio of Ni. If E is the width of the d band,

$$\frac{H_z^e}{E} = \tfrac{1}{5}\langle S_z \rangle \simeq \tfrac{1}{10}$$

as $\langle S_z \rangle$ is about 0·5 electron from saturation magnetization measurements. The spin–orbit term AL_zS_z changes the relative populations of the different m sublevels of the d bands:

$$\langle L_z \rangle = \sum_m L_z^2 \frac{A}{2E} = \frac{5A}{E}$$

$$\frac{\langle L_z \rangle}{\langle S_z \rangle} \simeq \frac{10A}{E} \simeq \frac{A}{H_z^e} = \epsilon.$$

Now $g' \simeq 2(1 - \langle L_z \rangle / \langle S_z \rangle) = 1·83$ for Ni (Scott and Sturner 1969), giving an estimate for $\gamma = 3\epsilon^2/4 \simeq 0·0075$, in surprisingly good agreement with the value deduced above.

7. Conclusion

This very simple model leads to formulae which give qualitative predictions for $\Delta\rho/\rho$ as a function of the nature of the impurity, the concentration and the temperature. These predictions are correct to the present accuracy of the experimental parameters; this precision is a further justification of the parallel current mechanism, and provides a very clear example of the influence of spin–orbit effects on transport properties.

More accurate values of α, $\mu(T)$ and $\rho_{\uparrow\downarrow}(T)$ are needed; it is to be hoped that it will be possible to separate $\rho_\downarrow$ for different impurities (and for phonons) into s–d and s–s processes. It is known that $\Delta\rho/\rho$ is anisotropic in single crystals; a careful study of this effect should provide information on the Fermi surface of Ni and on the scattering mechanisms.

References

BERGER, L., *Physica,* **30**, 1141–7.
CAMPBELL, I. A., 1970, *Phys. Rev. Lett.,* **24**, 269–71.
CAMPBELL, I. A., FERT, A., and POMEROY, A. R., 1967, *Phil. Mag.,* **15**, 977–83.
VAN ELST, H. C., 1959, *Physica,* **25**, 708–20.
FARRELL, T., and GREIG, D., 1968, *J. Phys. C: Solid St. Phys.,* **1**, 1359–69
FERT, A., and CAMPBELL, I. A., 1968, *Phys. Rev. Lett.,* **21**, 1190–2.
FERT, A., 1969, *J. Phys. C: Solid St. Phys.,* **2**, 1784–8.
FRIEDEL, J., 1958, *Nuovo Cim.,* **7**, Suppl. 2, 287–98.
GOMES, A. A., 1966, *J. Phys. Chem. Solids,* **27**, 451–63.
SCOTT, G. G., and STURNER, H. W., 1969, *Phys. Rev.,* **184**, 490–1.
SMIT, J., 1951, *Physica,* **17**, 612–22.
VU DINH KY., 1967, *Sov. Phys.–JETP,* **24**, 995–9.

F